Wan Noni Afida Ab Manan^{1,2} and Ahmad Zamani Ab Halim^{1*}

¹Faculty of Industrial Sciences and Technology, Universiti Malaysia Pahang Al-Sultan Abdullah, Lebuh Persiaran Tun Khalil Yaakob, 26300, Kuantan, Pahang, Malaysia ²Faculty of Applied Sciences, Universiti Teknologi MARA Pahang, Jengka Campus, 26400 Bandar Tun Abdul Razak Jengka, Pahang, Malaysia *Corresponding author (e-mail: ahmadzamani@umpsa.edu.my)

Activated carbon adsorption is an effective approach for removing textile dyes from wastewater, given its simplicity, efficiency, and high performance. The selection of adsorbents for the adsorption process contributes to the performance of the percent removal. Thus, the efficacy of chemically Activated Nanomagnetic Biochar (ANB) was investigated as an adsorbent. Three types of wood waste biomasses (oil palm trunk, pinewood, and rubberwood) were selected to synthesize ANB. The activation of biochar by phosphoric acid (H₃PO₄) introduced more pores, hence more surface area, leading to improved adsorption capacity. Additionally, chemical-Activated Biochar (AB) with magnetite (Fe₃O₄) was successfully synthesized via the coprecipitation technique and applied in Malachite Green (MG) dye removal. Fourier-Transform Infrared Spectroscopy (FTIR), as well as Brunauer-Emmett-Teller (BET) surface area, were employed to characterize the synthesis of ANB. The prepared adsorbent contains a high specific surface area of 78.9727 m²/g, 69.4350 m²/g, and 66.7358 m²/g for ANBO, ANBP, and ANBR, respectively. FTIR analyses show that the surface formed functional groups, which were aliphatic and carbonyl functional groups. The results indicated that ANBO removed MG with an efficiency above 87% compared to other adsorbents. The results suggested the ANBO can be utilized as an adsorbent to eliminate MG dye from the wastewater.

Keywords: Adsorption; adsorbent; ANB; dye removal; nanomagnetic

Received: April 2025; Accepted: August 2025

The discharge of synthetic dyes from various industries, including cosmetics, food, printing, textiles, and electroplating, substantially adds to water pollution, endangering aquatic ecosystems [1]. Dyes, due to their toxic properties, present significant environmental hazards and adversely affect human health upon consumption [2]. According to Jamiu et al. [3], the use of various types of dyes is increasing significantly across various industries, resulting in an annual

production of synthetic dyes exceeding 2 x 10⁵ metric tons [3]. Malachite Green (MG) is a triphenylmethane dye that has been applied around the world in aquaculture since the 1930s for its antimicrobial as well as antiparasitic properties. It is organic, water-soluble, and cationic. MG is one of the notable dyes of concern [1, 4]. The chemical structure of MG demonstrates the presence of three benzene rings, with the molecular formula C₂₃ H₂₅ClN₂. Figure 1 illustrates MG's chemical structure.

Figure 1. Chemical structure of malachite green dye [5, 6].

69

Synthesis, Characterization, and Adsorption Screening of Nanomagnetic Activated Carbon Derived from Biomass Waste: Oil Palm Trunk, Pinewood, and Rubberwood for the Removal of Malachite Green Dye Solution

The wide application concerning MG dye has resulted in its introduction into the food chain, where it exposes humans and animals to its teratogenic, carcinogenic, as well as mutagenic impacts due to direct contact, inhalation, or even ingestion [7]. Therefore, it is important that MG be removed from industrial effluents prior to their disposal in aquatic settings.

Effluent containing dyes can be treated using many methods, such as physical (membrane filtration, coagulation-flocculation, and adsorption), biological, as well as chemical (advanced oxidation processes) treatment techniques [1, 2]. However, each of these wastewater treatment technologies is associated with significant drawbacks, including the generation of substantial volumes of secondary pollutants and high costs [3]. Relatively, adsorption is considered the most effective and sophisticated method for eliminating contaminants from real water, due to its simple design, cost-effectiveness, and high performance compared to other methods [3 - 5]. Activated carbon is the most utilized material for adsorbing inorganic as well as organic pollutants from wastewater, given its rapid adsorption kinetics and high surface area. However, the use of commercial activated carbon is constrained by the high production costs of raw materials, such as coal, and challenges associated with regeneration [3, 4, 6]. These limitations have prompted researchers to seek low-cost, renewable, abundant, and highly efficient adsorbents, including natural and waste materials, while also exploring more economical production methods for activated carbon materials [6].

Agricultural waste was identified as a low-cost and efficient source of sustainable adsorbents in the decontamination of the wastewater [4]. Several ways of improving pore volume porosity, as well as surface area, concerning agricultural wastes were documented [8]. This is done by surface modification, either by carbonization (physical activation) or by the use of salts (chemical activation), bases, as well as acids [4]. The utilization concerning biomass waste in wastewater treatment is recognized as a method for converting

waste into valuable resources. The research performed by Zakaria et al. [9] investigated the effectiveness of activated carbon derived from coconut shells in removing MG dye, revealing a remarkable 99% removal rate of the dye. Mohamad et al. [8] achieved a similar outcome using Jackfruit Peel-based Activated Carbon (JPAC) regarding the MG dye treatment from aqueous solutions, resulting in a 66.80 mg/g adsorption capacity concerning MG.

Biochar, a carbonaceous solid substance formed from biomass through thermochemical conversion in the absence or limited presence of oxygen, is recognized as a highly promising adsorbent [10]. Nevertheless, the recovery of biochar after its use in aqueous solutions is challenging due to its small size [11] and when attempting to separate components in powdered form [12]. Therefore, biochar with magnetization capabilities has been utilized to enhance the efficacy of water treatment processes, demonstrating promising results for pollutant removal and facilitating easy separation from solutions via magnetic separation [13]. Nevertheless, there are a few research in the literature regarding the adsorption performance of coprecipitated nanomagnetic materials. Magnetic sorbents, specifically magnetite iron oxide nanoparticles (Fe₃O₄), were employed in agricultural waste to address these constraints. These nanoparticles enhance surface area, reactivity, adsorption efficiency, and reusability, while concurrently reducing the intraparticle diffusion rate [14]. Table 1 presents a selection of previous studies that utilized magnetic biochar on agricultural waste with regard to the MG dye pollutant removal in wastewater.

This study's primary aim is to evaluate the feasibility regarding removing MG dye from wastewater utilizing different types of wood waste as adsorbent agents. Magnetic biochar containing Fe₃O₄ was synthesized from wood waste-derived biochar as well as ferric salt solution via the coprecipitation method. Note that the adsorption screening was applied to determine the best adsorbent for MG dye removal.

Magnetic biochar	Synthesis method	Efficiency (%)	Reference
Peanut hull	coprecipitation	95	[15]
Bamboo fiber tissue	mixing montmorillonite loaded with trioxide and acrylic acid- modified	97.3	[16]
Sunflower husk	Pyrolysis and hydrothermal carbonization	77 and 82.18	[17]
Tamarindus indica fruit seed	Pyrolysis	88.36	[18]
Corn straw	Chemical Reduction	99	[19]

MATERIALS AND METHODS

Materials

Waste biomass was obtained from the residual waste produced during wood production that the factory intends to remove. Three types of wood biomass were selected: pinewood (Pinus), rubberwood (Hevea brasiliensis), and oil palm trunk (Elaeis guineensis). The wood biomass was processed into smaller pieces through chopping and chipping. Subsequently, it will be screened to achieve particle sizes of 1-1.5 mm and air-dried prior to grinding into smaller particles ranging from 200 to 400 µm. The sieved materials underwent several rinses with distilled water and were subsequently dried in a convection oven at 70°C overnight.

The chemicals: Iron (II) chloride tetrahydrate (FeCl₂.4H₂O) 99%, Iron (III) chloride hexahydrate (FeCl₃.6H₂O) 97%, phosphoric acid (H₃PO₄) 85%, hydrochloric acid (HCl) 37%, sodium hydroxide (NaOH), as well as nitric acid (HNO₃) were acquired from Sigma-Aldrich. MG dye was purchased from R&M Chemicals.

Preparation of MG Dye Solution

A 1000 mg/L MG stock solution was arranged by dissolving 0.1 g concerning MG in a 100 mL volumetric flask using distilled water. Serial dilution was utilized to produce standard solutions with lower concentrations from the 1000 mg/L stock solution. A UV-Vis spectrophotometer (UV-1800, Shimadzu, Japan) was utilized at $\lambda_{max} = 617$ nm to ascertain the final concentrations of the prepared standards. Three standard concentrations of MG (5, 10, and 15 mg/L) and a blank (distilled water) were utilized for subsequent analysis.

Synthesis of Activated Nanomagnetic Biochar (ANB)

The Activated Nanomagnetic Biochar (ANB) was synthesized using a two-step method, as modified by Ayob et al., Venkata et al., Bijoy et al., Norbert et al., Najmeh et al., and Mary et al. [20 - 25]. The initial step involved placing wood biomass in a pyrolysis process following the TGA test under nitrogen atmosphere with a 10°C/min heating rate, having temperatures ranging from 30 - 1000°C. Consequently, the temperature of the furnace depended upon the results of the test. The pyrolysis process took approximately 2 hours, followed by cooling to room temperature.

Chemical activation regarding biochar was done following the procedure described by Wipawee and Attaso [26] with some modifications made. A finely ground biochar of 2 g was put in 85% v/v H₃PO₄ containing 300 ml. The acid was used to immerse the biochar for a period of 24 hours.

Synthesis, Characterization, and Adsorption Screening of Nanomagnetic Activated Carbon Derived from Biomass Waste: Oil Palm Trunk, Pinewood, and Rubberwood for the Removal of Malachite Green Dye Solution

Consequently, the Activated Biochar (AB) was washed using distilled water until it reached a pH of 7. The AB was subsequently dried in an oven at 105°C for a duration of 24 hours.

ANB synthesis was carried out utilizing the chemical coprecipitation method, following the prescribed procedure by Ayob et al., Venkata et al., Bijoy et al., Norbert et al., Najmeh et al., and Mary et al. [20 - 25]. The synthesis of Fe₃O₄ nanoparticles was accomplished using dissolved hydrate compounds, namely Iron (III) chloride hexahydrate (FeCl₃.6H₂O) as well as Iron (II) chloride tetrahydrate (FeCl₂.4H₂O). These compounds provide Fe³⁺ and Fe²⁺ ions in a mass ratio of 2:1, respectively [21]. Note that 1 g concerning AB was dispersed in distilled water at 80°C, containing 200 mL. After 10 minutes, 4.72 g of FeCl₃.6H₂O as well as 2.36 g of FeCl₂.4H₂O were added. Consequently, the solution underwent heating at 80°C for 30 minutes while being stirred magnetically at 100 rpm. After an increment in stirring to 1000 rpm, ammonia (NH₃) was added drop by drop to raise the pH to 10 [24]. The solution was heated to 80°C and kept there at 100 rpm of stirring during a period of 1 hour. The solid was filtered off a permanent magnet as well as washed with 100 mL of ethanol and 2 L of distilled water until pH approached neutrality and dried for 24 hours at 100°C [27]. This deposition process utilized the magnetic field generated by a permanent magnet to enhance efficiency [23]. The ANB for each type of wood biomass was assigned according to the labelling scheme specific to each category, including ANBP (pinewood), ANBR (rubberwood), and ANBO (oil palm trunk).

Characterization

The adsorbent was analyzed using FTIR to determine any potential functional groups present. Brunauer-Emmett-Teller (BET) was implemented to measure the specific surface area of AB and ANB. The precisely weighed AB and ANB (± 0.04 g) were degassed at 100°C and adsorbed under N₂ at 77 K.

Adsorption Experiment Screening

The aim is to identify the wood biomass type that exhibits the highest removal efficiency. The initial adsorption screening was conducted at a constant pH of 8 and a fixed temperature of 25°C. Two different dosages, 0.02 g and 0.03 g, were applied to determine the effect of dosage. The experiments were carried out utilizing a 100 mL Erlenmeyer flask filled with ANB and 50 mL of a 10 mg/L solution of MG at room temperature. Note that the mixture was incubated on an incubator shaker at 100 rpm for 1 hour, and the remaining MG concentration was examined utilizing a UV-Vis Spectrophotometer.

The amount of dyes adsorbed onto asprepared adsorbents q_e (mg/g) as well as its adsorption performance (%) were computed from the equation by Goudu et al. [28] as follows:

$$q_{e=\frac{(C_O-C_E)}{M}}v,\tag{1}$$

$$\% R = \frac{(c_o - c_e)}{c_o} \times 100\%, \tag{2}$$

in which q_e (mg/g) refers to the adsorption capacity of metals onto absorbents, % R is the adsorption performance of metals onto absorbents, C_o and C_e represent initial and equilibrium concentrations of dyes (mg/L), respectively. V resembles the aqueous solution volume (L), while M denotes the amount of adsorbents (g).

The rate of adsorption was studied with the help of Pseudo-First Order (PFO) as well as Pseudo-Second Order (PSO) kinetic models. The linear form regarding the PFO and PSO kinetic models is shown in equations (3) as well as (4), correspondingly [29]:

$$\ln q_e - q_t = \ln q_e - \frac{k_1 t}{2.303'} \tag{3}$$

$$\frac{t}{q_t} = \frac{1}{k_2 q_e^2} + \frac{1}{q_e} t,\tag{4}$$

in which q_t represents the adsorption amounts (mg. g^{-1}) of the adsorbate at a specified time t (min). k_1 (min⁻¹) and k_2 (g (mg⁻¹ min⁻¹)) refer to the respective rate constants.

The adsorption isotherm serves as a tool for evaluating the adsorption capacity and elucidating the interaction between MG and the adsorbents. This study analyzed the MG adsorption equilibrium in an aqueous solution utilizing the Langmuir (equation (5)) as well as the Freundlich (equation (6)) isotherm models [30]:

$$\frac{c_e}{q_e} = \frac{1}{q_m k_L} + \frac{c_e}{q_m},\tag{5}$$

$$\ln q_e = \ln k_F + \frac{1}{n} \ln c_e \,, \tag{6}$$

where q_m (mg/g) denotes the theoretical maximum adsorption capacity; k_L (L/mg) and k_F (L/mg) represent the Langmuir as well as the Freundlich model isotherm constants, n signifies the dimensionless constant concerning the Freundlich model, respectively.

Synthesis, Characterization, and Adsorption Screening of Nanomagnetic Activated Carbon Derived from Biomass Waste: Oil Palm Trunk, Pinewood, and Rubberwood for the Removal of Malachite Green Dye Solution

RESULTS AND DISCUSSION

Fourier Transform Infrared Analysis (FTIR)

FTIR analysis was conducted to determine the functional groups present on the surfaces of ANBO, ANBP, and ANBR compared with their raw biomasses and biochar, as depicted in Figure 2. The band observed between 3000 and 3500 cm⁻¹ is attributed to the stretching mode of hydroxyl groups (-OH) in all FTIR spectra. The absorption peaks at 1,631 cm⁻¹ as well as 1,380 cm⁻¹ correspond to C=O and C-O telescopic vibrations, correspondingly [15]. ANBO, ANBP, and ANBR showed strong absorption bands at 554 and 564 cm⁻¹ that were attributed to the Fe-O vibration of the magnetite phase. FTIR spectra show that in the presence of magnetite nanoparticles in the carbon-based matrix, the bands regarding the magnetic carbonaceous materials shift slightly with variations in the intensity, especially in the O-H as well as C=C stretching vibration. The observation indicates that there exists an interaction between the carbonaceous materials as well as the magnetite nanoparticles [17]. This indicates that the material's surface is characterized by the presence of hydroxyl groups, carboxyl groups, and Fe-O bonds, which facilitate the removal of pollutants in its role as an adsorbent [15].

Brunauer-Emmett-Teller (BET) Surface Area and Porosity

The surface area as well as the size of pores of the adsorbent have a substantial effect on the adsorption capacity of the adsorbent [31]. As a result, one should consider structural parameters such as surface area and porosity using the BET adsorption technique [14]. The data on the pore volume, BET surface area, as well as pore diameter of AB and ANB were presented in Table 2. Burbano et al. [17] state that thermochemical processing of lignocellulosic biomass, in the form of pyrolysis or hydrothermal carbonization, entails a dehydration reaction. The reaction enables the removal of volatile components of the carbon matrix, which also leads to the formation of a porous structure. Note that Table 2 indicates that ANBO has a high BET surface area as well as high porosity, which are 78.97 m²/g and 0.23 cm³/g, correspondingly. On the other hand, ABR possesses a low BET surface approximately 27.62 m²/g. The observed difference can be attributed to the incorporation of magnetite nanoparticles into the carbon matrix of ANB material, which is advantageous for increasing the BET surface area. This result also side-steps the success of preparation of ANB material [31].

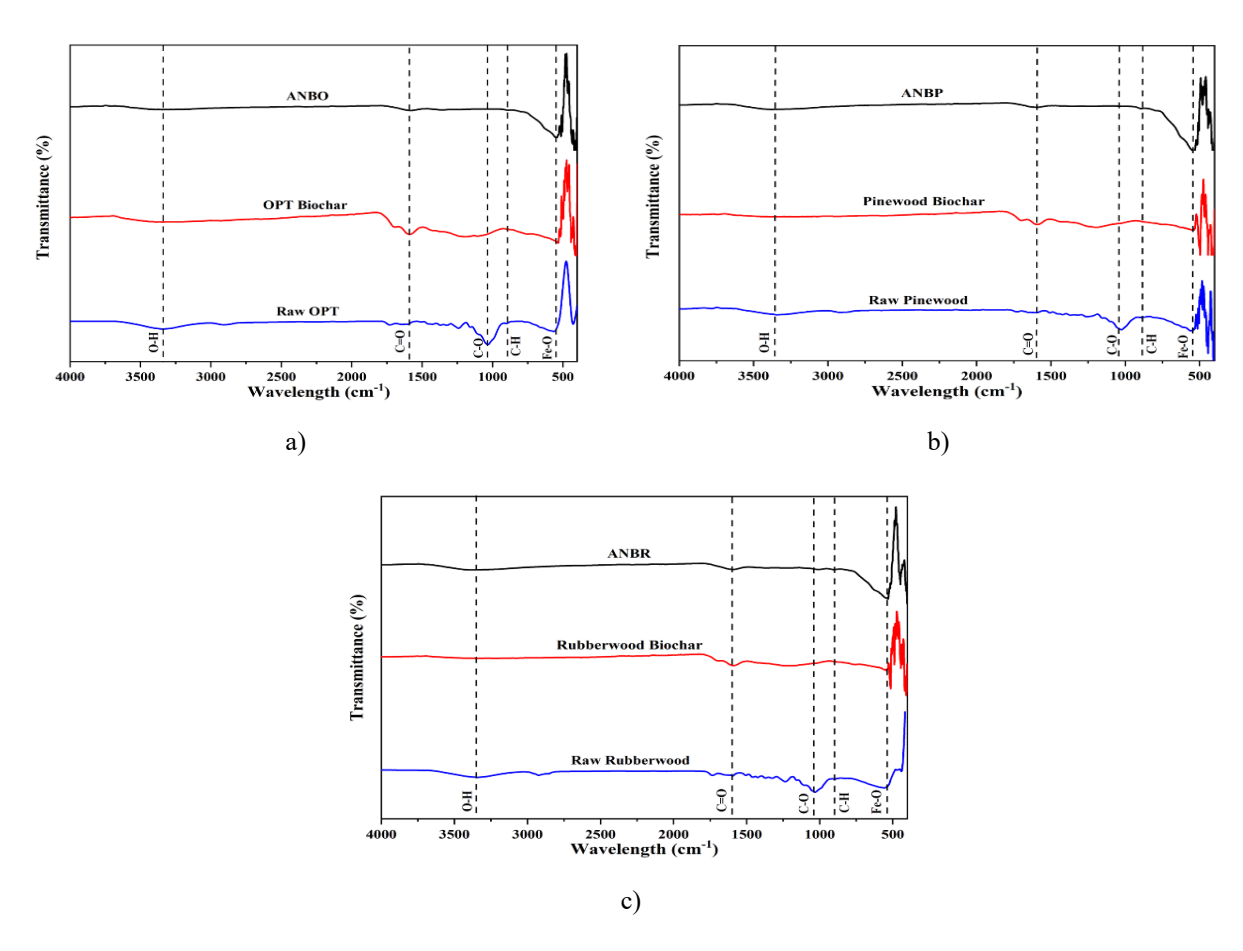


Figure 2. FTIR for raw, biochar, and ANB of a) Oil Palm Trunk, b) Pinewood, and c) Rubberwood.

Table 2. SBET.	, pore volume, as well	as pore diameter of AB and ANB.
----------------	------------------------	---------------------------------

Materials	$S_{BET}(m^2/g)$	Pore volume (cm³/g)	Pore diameter (Å)
ABO	58.39	0.06	43.88
ABP	37.81	0.05	54.91
ABR	27.62	0.05	70.82
ANBO	78.97	0.23	117.17
ANBP	69.44	0.21	119.51
ANBR	66.74	0.23	135.09

Figure 3 shows the fitting of the N₂ adsorptiondesorption isotherm, surface area as well as pore diameter of the AB and ANB. The curves show that the adsorption isotherms are type IV in general (Figure 3 (b, c, d, e, and f). The adsorption isotherm of Figure 3 (a) was more of a type II. Type II isotherm is due to uninhibited monolayermultilayer adsorption when the p/p⁰ levels are

high. A gradual bend at the lower p/p⁰ end implies a significant overlap of the monolayer coverage and the onset of the multilayer adsorption [32]. Mesoporous adsorbents are usually correlated with type IV isotherms. The adsorption in mesopores depends on the interactions of the adsorbent and adsorptive and interactions of molecules in the condensed phase [33].

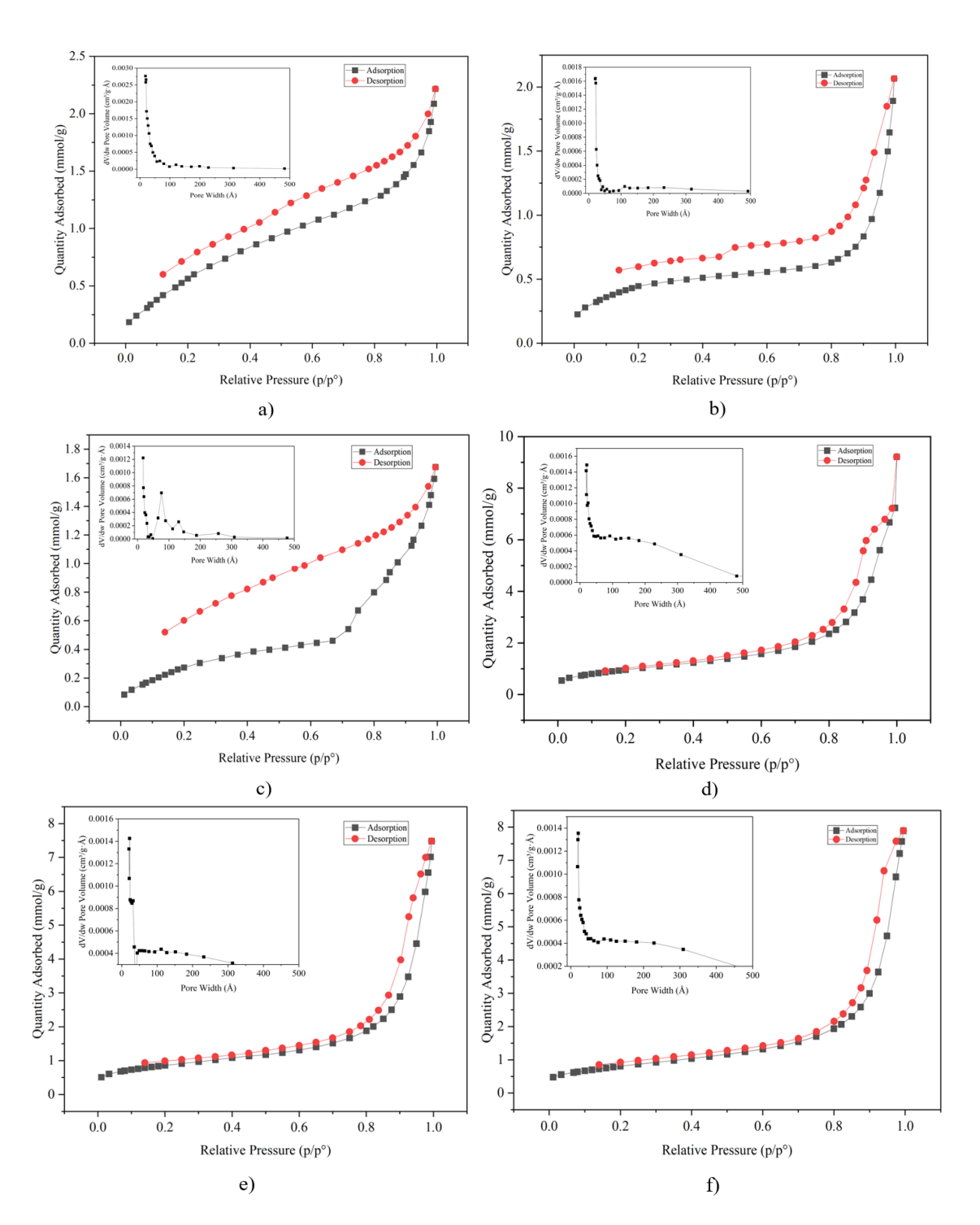


Figure 3. N₂ adsorption—desorption isotherms as well as Barrett-Joyner-Halenda (BJH) pore size distribution curves (inset) of (a) ABO, (b) ABP, (c) ABR, (d) ANBO, (e) ANBP, (f) ANBR.

Batch Sorption Screening

To have a preliminary understanding of the removal ability of the adsorbent prepared in this study, MG dye was selected as the adsorbate to study the removal efficiency of different adsorbents. The comparison of the removal efficiency of the three ANBs is shown in Figure 4. The effect of adsorbent dosage on the adsorption of MG dye showed that the removal efficiency for MG dye increased with an increase in

adsorbent dosage. The removal ability of MG on ANBO was higher than that of ANBP and ANBR by $87 \pm 11.5\%$ for a 0.03 g dosage. According to Mohamad et al. [34], the quantity of sorption sites on the adsorbent surface increases with a higher dose of the adsorbent. At low adsorbent dosage (0.02 g), the adsorbent surface becomes saturated with the MG dye, and the residual dye concentration in the solution is high. These two dosages were chosen due to their removal efficiency exceeding 50%. Modified wood

biomass offers several benefits in the adsorption process. Biomass waste is a cost-effective resource that can contribute to green chemistry processes by optimizing energy consumption and minimizing environmental impact. The adsorbent can be efficiently and rapidly separated from the dye solution using an external magnet. Furthermore, the magnetization exhibited a synergistic effect on dye adsorption due to the increased polarity of Fe-O in magnetite [35]. Above all, the magnetization by the coprecipitation method enhanced the uptake of MG dye, and when compared to different adsorbents, ANBO suggests the great potential of ANB-type materials in MG dye removal from aqueous solutions.

Selective Adsorption Analysis

Figure 5 indicates the selective dye adsorption of ANBO. The color of the residual solution of the MG dye varied between blue, which was present at the start of the adsorption process, and light blue, which was present at the end of the adsorption process, as illustrated in Figure 5(a). The corresponding UV-Vis spectra showed that the absorption peak of MG at λ_{max} = 617 nm was decreased remarkably after adsorption (Figure 5 (b)). This was primarily because of the high electrostatic force that existed between the cationic dye and the ANBO, which was negatively charged [16]. This meant that ANBO had a good adsorption effect on cationic dye, particularly on MG.

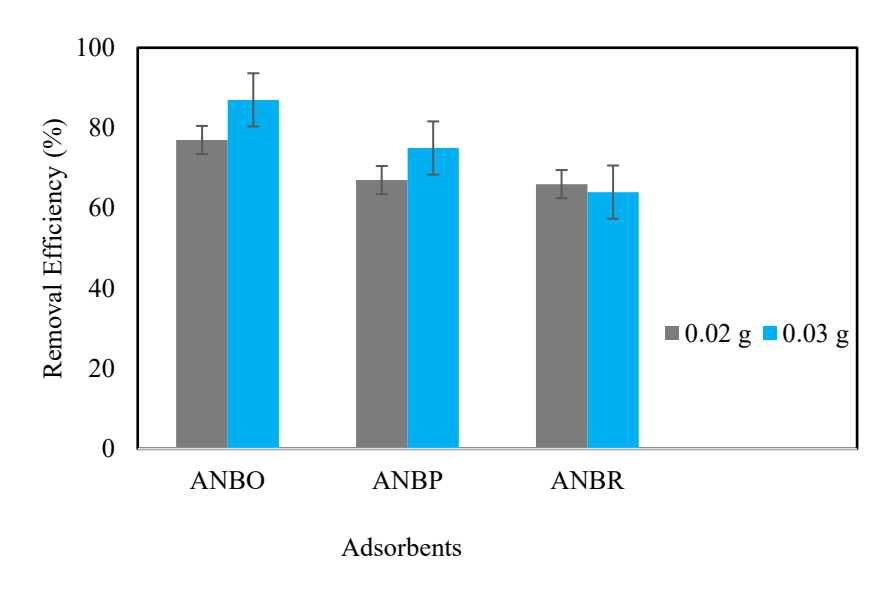


Figure 4. Comparison of ANBs with different dosages for MG dye removal.

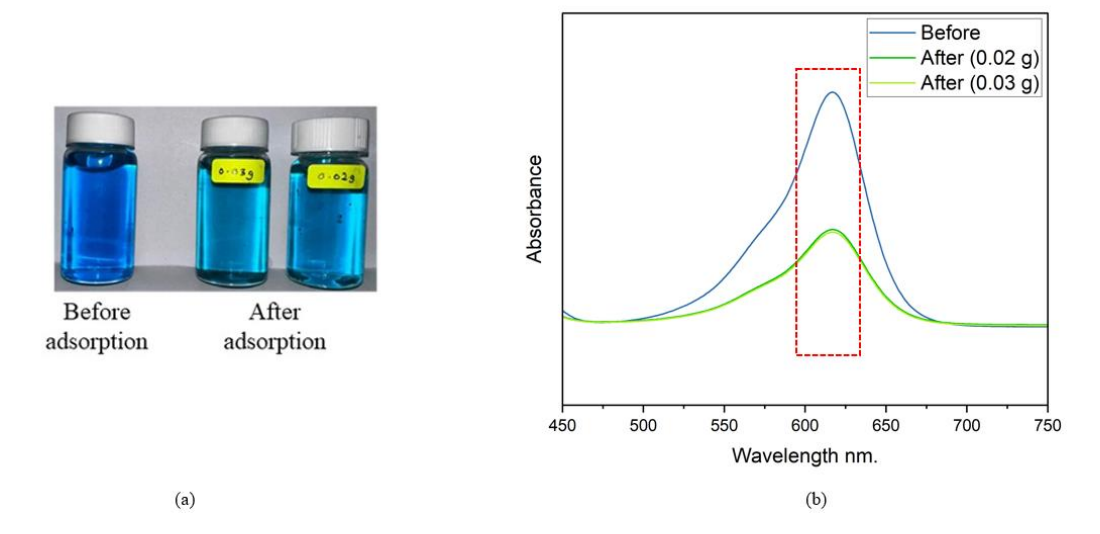


Figure 5. Changes of MG before and after adsorption (a) photograph color changes and (b) UV-Vis spectra.

Adsorption Kinetics and Isotherm Studies

To improve the knowledge regarding the adsorption process and the mechanism of interaction between MG and the adsorbent, adsorption kinetics and adsorption isotherms of MG on ANBO were studied. The fitting curves concerning three models were shown in Figure 6 under various MG initial concentrations. The kinetic parameters with regard to PFO as well as PSO models were summarized in Table 3. The R² values regarding the PSO kinetic model (0.99997, 0.99994, and 0.9999 for initial concentrations of 5, 10, and 15 mg/L, correspondingly) were substantially greater compared to those of the PFO kinetic model (0.01203, 0.436936, as well as 0.71558 for initial concentrations of 5, 10, and 15 mg/L, correspondingly), regardless of

the MG initial concentration. Furthermore, the qe (cal.) values derived from the PSO kinetic model (3.216572, 6.262, 9.489 mg/g) were closer to the experimental q_e (exp.) values (3.249, 6.33, 9.55 mg/g) than those calculated from the PFO kinetic model (0.075217, 0.173283, 0.305215 mg/g, correspondingly). Note that the PSO kinetic model is more appropriate for describing the adsorption process of MG by ANBO. The analysis findings reveal that the adsorption of MG by ANBO is mostly chemical adsorption as well as the effectiveness regarding adsorption primarily depends on the adsorption sites concerning biochar. The findings align with the earlier report by Ahmad et al. [30], who also synthesized MgAlLDH-magnetite humic acid (Mg3Al@M2HA) and determined that the PSO model fitted better on the kinetic model than the PFO model.

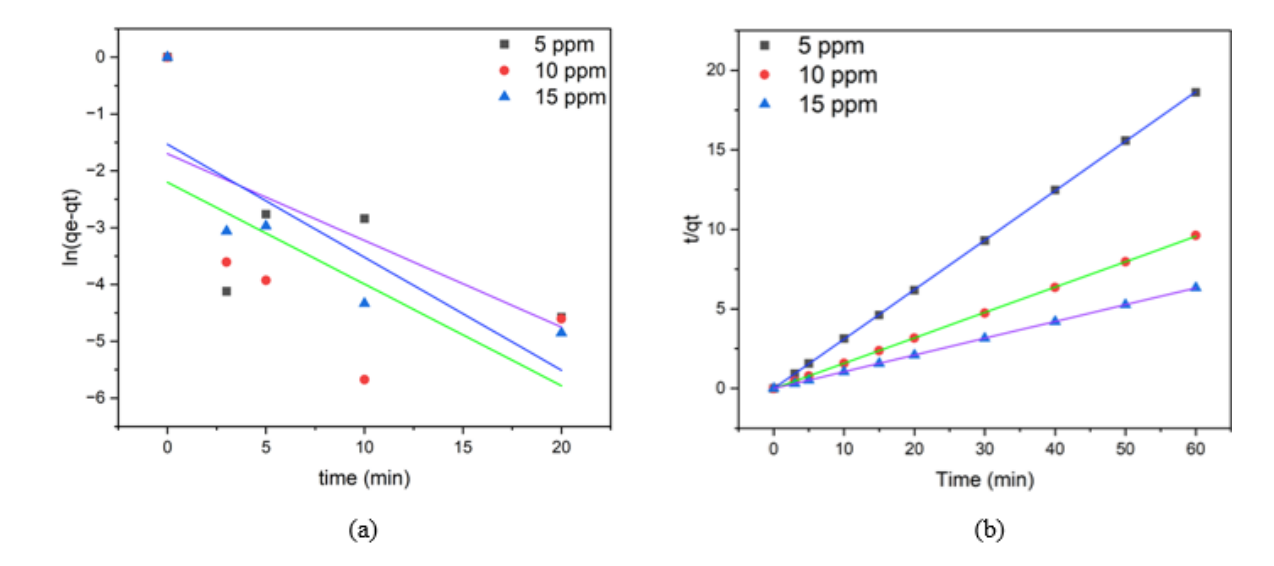


Figure 6. The fitting of (a) the PFO model and (b) the PSO model for MG adsorption onto ANBO at 298 K.

Table 3. Kinetic parameters of PFO and PSO for MG adsorption by ANBO under different concentrations.

Model	Parameters	Initial MG concentration (c_o) (mg/L)		
	•	5	10	15
Experimental	q _e (mg/g)	3.249	6.33	9.55
Pseudo-first order (PFO)	$q_e \left(mg/g \right)$	0.075217	0.173283	0.305215
	$K_1(min^{-1})$	0.009566	0.119036	0.122145
	\mathbb{R}^2	0.01203	0.436936	0.71558
Pseudo-second order (PSO)	$q_e \ (mg/g)$	3.216572	6.262	9.489
	K ₂ (min ⁻¹)	-20.5207	-1.42481	-2.29441
	\mathbb{R}^2	0.99997	0.99994	0.9999

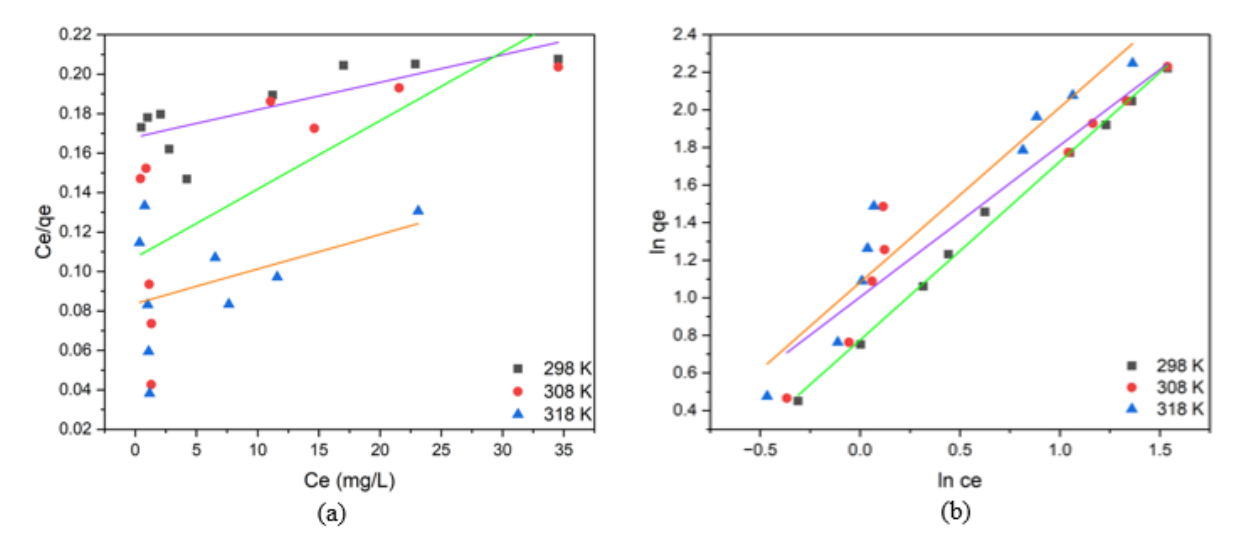


Figure 7. Plots of (a) Langmuir isotherm and (b) Freundlich isotherm for the adsorption of MG by ANBO at different temperatures.

Table 4. Adsorption isotherm constants concerning MG adsorption onto ANBO at various temperature.

Temperature (K)	Langmuir isotherm constants			Freundlich isotherm constants		
	$q_m (mg/g)$	$k_L(L/mg)$	R^2	$k_F (L/mg)$	1/n	R^2
298	719.424	0.008269	0.575	5.965	0.94917	0.995
308 318	288.184 571.429	0.03243 0.020903	0.465 0.058	10.088 12.073	0.80759 0.93166	0.890 0.912

Different isotherm models have been used to interpret the data obtained in adsorption experiments [19]. The study utilized the Langmuir and the Freundlich models for analysis. Figure 7 illustrates the isotherms of MG adsorption on ANBO at various temperatures. The calculated theoretical maximum adsorption capacities (q_m) for MG on ANBO, derived from the Langmuir model, were 719.424 mg/g, 288.184 mg/g, and 571.429 mg/g, respectively. The Freundlich model provided a superior representation of the removal process of MG by ANBO compared to the Langmuir model, as evidenced by the higher R² value. This suggests the occurrence of multilayer non-homogeneous physisorption behavior [36]. Additionally, the 1/n values were less than 1, suggesting that the MG adsorption process was favorable (refer to Table 4). The findings align with the earlier report by Yalvac et al. [37], which also indicated that the Freundlich isotherm, exhibiting an R² value of 0.997, was the most appropriate model among those tested for the adsorption of MG with Carbonized Mandarin Peel (CMP). The data show that the adsorption process is endothermic in nature.

CONCLUSION

In conclusion, this study effectively demonstrated the successful synthesis of chemically AB with Fe₃O₄ using the coprecipitation technique, which was implemented to eliminate MG dye. In MG adsorption, ANBO was determined to be the most effective adsorbent, and this might be because of its higher surface area than the other adsorbents. The results show that the new approach to making magnetic biochar is feasible, which makes it cost-effective in the context of wastewater treatment because of the increased capacity of adsorbents to leave their liquid phase. In addition, the obtained adsorbent portrayed a large adsorption capacity, which shows that it can be used as a good alternative in water contaminant remediation. Moreover, the utilization of wood biomass ensures cost-effectiveness and a sustainable way of managing solid wastes that would otherwise pose environmental issues when they are left to pile up in the environment.

ACKNOWLEDGEMENT

The authors thank and acknowledge the funding from the Ministry of Higher Education (MoHE), Malaysia, under the Skim Latihan Akademik Bumiputera (SLAB) for the financial support. The authors also wish to express their gratitude for the services and facilities provided by UiTM Pahang Branch and UMPSA to facilitate the laboratory work.

The authors declare that they have no conflict of interest.

REFERENCE

- 1. Devlina, D. P., Pratham, G., Divya, G. and Arindam, P. (2024) Removal of malachite green from an aqueous environment using chitosan-xanthan gum coagulation system: a response surface methodology approach. *Journal of Water Process Engineering*, **65**, 105896.
- Teeyasha, D., Animesh, D. and Mriganka, S. M. (2024) Adsorption of malachite green by Aegle marmelos-derived activated biochar: novelty assessment through phytotoxicity tests and economic analysis. *Journal of the Indian Chemical Society*, 101, 101219.
- 3. Jamiu, M. J., Matthew, A. A., Yisau, A. O., Murat, Y. and Selvasembian R. (2023) Valorization of microwave-assisted H₃PO₄-activated plantain (*Musa paradisiacal* L) leaf biochar for malachite green sequestration: models and mechanism of adsorption. *Results in Engineering*, **18**, 101129.
- Adewumi, O. D., Abosede, A. I., Blessing, E. T., Abiodun, A. B., Kehinde, S. O., Christina, O. A., Folahan, A. A., Kolawole, O. A. and Ujjwal, P. (2024) Zinc oxide decorated plantain peel activated carbon for adsorption of cationic malachite green dye: mechanistic, kinetics and thermodynamics modeling. *Environmental* Research, 252, 119046.
- Youssef, A. E. H. A., Lamia, H., Nordin, B. S., Abdelmonaim, A., Luis, P.-V., Mostafa, S. and Christian, S. (2024) Remediation of malachitegreen dye from textile wastewater using biosorbent almond shell-based cellulose. *Journal* of Molecular Liquids, 399, 124435.
- 6. Jari, S. A., Mohsen, A. M. A., Ayoub, A. A., Saad, M. and Amal, F. S. (2024) Magnetic hydrochar grafted chitosan for enhanced efficient adsorption of malachite green dye from aqueous solutions: modeling, adsorption behavior, and mechanism analysis. *International Journal of Biological Macromolecules*, **254**, 127767.
- 7. Rehab, E. E., Hassan, S., Ahmed, A. M. and Alaa, E. A. (2023) Influence of the prepared activated carbon on cellulose acetate for malachite green dye removal from aqueous solution. *Macromolecular Research*, **31**, 1043–1060.
- 8. Mohamad, F. M. Y., Ahmad, Z. A. and Mohd, A. A. (2023) Malachite green dye adsorption by jackfruit based activated carbon: optimization, mass transfer simulation, and surface area

- Synthesis, Characterization, and Adsorption Screening of Nanomagnetic Activated Carbon Derived from Biomass Waste: Oil Palm Trunk, Pinewood, and Rubberwood for the Removal of Malachite Green Dye Solution
 - prediction. *Diamond & Related Materials*, **136**, 109991.
- 9. Zakaria, W. A. N., Ghazi, R. M., Muhammad, M. And Jani, M. (2021) Optimization of malachite green removal using activated carbon derived from coconut shell. *Earth and Environmental Science*, **842**, 012033.
- 10. Na, Z., Febelyn, R., Sai, P. and Ajit, K. S. (2023) A green approach of biochar-supported magnetic nanocomposites from white tea waste: production, characterization, and plausible synthesis mechanisms. *Science of the Total Environment*, 886, 163923.
- 11. Xinxin, Y., Lili, J., Jian, G., Shaoliang, G., Wencheng, L., Lu, C., Yaning, W., Wendong, S. and Hailong, Z. (2020) Magnetic activated biochar nanocomposites derived from wakame and its application in methylene blue adsorption. *Bioresource Technology*, **302**, 122842.
- 12. Jayanthi, B., Palsan, S. A. and Emenike, C. U. (2022) Application of magnetic carbon nanocomposite from agro-waste for the removal of pollutants from water and wastewater. *Chemosphere*, **305**, 135384.
- Zhihong, Y., Yunguo, L., Shaobo, L., Luhua, J., Xiaofei, T., Guangming, Z., Meifang, L., Sijia, L., Sirong, T. and Ying, F. (2018) Activated magnetic biochar by one-step synthesis: enhanced adsorption and coadsorption for 17β-estradiol and copper. Science of the Total Environment, 639, 1530–1542.
- 14. Venkata, S. M., Hsin-Yu, W., Anjani, R. K. G., Jet-Chau, W., Kun-Yi, A. L., Chi-Min, S., Vijaya, Y., Praveen, K. B., Guda, M. R. and Grigory, V. Z. (2023) Magnetic Fe3O4 nanoparticles loaded guava leaves powder impregnated into calcium alginate hydrogel beads (Fe3O4-GLP@CAB) for efficient removal of methylene blue dye from aqueous environment: synthesis, characterization, and its adsorption performance. *International Journal of Biological Macromolecules*, 246, 125675.
- Xiaohui, Z., Qiong, H., Chengyu, W., Xiaodan, W., Hongpei, Z., Ke, Z., Binguo, Z., Jinwen, Y. and Junling, N. (2023) Study on adsorption performance and mechanism of peanut hullderived magnetic biochar for removal of malachite green from water. *Materials Research Express*, 10, 095504.
- Xuelun, Z., Chongpeng, Q., Feng, L., Xuefeng,
 Z., Mei-Chun, L., Jiulong, X., Cornelis, F. D.
 H., Jinqiu, Q. and Xingyan, H. (2023) Magnetic nanocellulose-based adsorbent for highly selective

- Synthesis, Characterization, and Adsorption Screening of Nanomagnetic Activated Carbon Derived from Biomass Waste: Oil Palm Trunk, Pinewood, and Rubberwood for the Removal of Malachite Green Dye Solution
- removal of malachite green from mixed dye solution. *International Journal of Biological Macromolecules*, **253**, 126752.
- 17. Burbano, A. A., Gascó, G., Horst, F., Lassalle, V. and Méndez, A. (2023) Production, characteristics, and use of magnetic biochar nanocomposites as sorbents. *Biomass and Bioenergy*, **172**, 106772.
- Okan, B., Emel, M., Elif, K., Fethiye, G. and Erol, P. (2023) Removal of methyl blue and malachite green from water using biodegradable magnetic *Tamarindus Indica* fruit seed biochar: characterization. Equilibrium study, modelling and thermodynamics. *Sustainable Chemistry for* the Environment, 3, 100023.
- Eltaweil, A. S., Mohamed, H. A., Eman, M. A. E., El-Subruiti, G. M. (2020) Mesoporous magnetic biochar composite for enhanced adsorption of malachite green dye: characterization, adsorption kinetics, thermodynamics and isotherms. *Advanced Powder Technology*, 31, 1253–1263.
- Ayoub, A. A., Moonis, A. K., Marta, O., Masoom, R. S., Byong-Hun, J. and Khalid, M. B. (2018) A magnetic nanocomposite produced from camel bones for an efficient adsorption of toxic metals from water. *Journal of Cleaner Production*, 178, 293–304.
- Venkata, S. M., Hsin-Yu, W., Anjani, R. K. G., Jet-Chau, W., Chi-Min, S., Kun-Yi, A. L., Zhong, T., Jhy-Horng, W., Guda, M. R. and Grigory, V. Z. (2022) Magnetic Fe₃O₄ nanoparticles loaded papaya (*Carica* papaya L.) seed powder as an effective and recyclable adsorbent material for the separation of anionic azo dye (Congo Red) from liquid phase: evaluation of adsorption properties. *Journal of Molecular Liquids*, 345, 118255.
- 22. Bijoy, B., Tawsif, R., Manish, S., Hossein, J., Mohamed, E., Jonas, B., Jasmeer, L., Allen, T. and Sushil, A. (2023) Phosphorus adsorption using chemical and metal chloride activated biochars: isotherms, kinetics and mechanism study. *Heliyon*, **9**, e19830.
- 23. Norbert, O. R., Marwa, E., Ahmed, E., Manabu, F., Sekiguchi, H. and Hassan, S. (2023) Effective decontamination of methylene blue from aqueous solutions using novel nanomagnetic biochar from green pea peels. *Environment Research*, **220**, 115272.
- 24. Najmeh, K., Amin, M., Mohammad, R. S., Ali, M. A., Mansooreh, D., Rajender, S. V. and Sahu, J. N. (2024) Green synthesis of sustainable magnetic nanoparticles Fe₃O₄ and Fe₃O₄-chitosan derived from Prosopis farcta biomass

- extract and their performance in the sorption of lead (II). *Inter-national Journal of Biological Macromolecules*, **254**, 127663.
- 25. Mary, M., Hamza, A. and Chirangano, M. (2024) Turning teawaste particles into magnetic biosorbents particles for arsenic removal from wastewater: isotherm and kinetic studies. *Particuology*, **87**, 179–193.
- 26. Wipawee, D. and Attaso, K. (2023) Biosorption of aqueous Pb (II) by H₃PO₄-activated biochar prepared from palm kernel shells (PKS). *Heliyon*, **9**, e17250.
- 27. Joanna, D., Anna, W. and Rafal, O. (2022) Raspberry stalks-derived biochar, magnetic biochar and urea modified magnetic biochar synthesis, characterization, and application for As (V) and Cr (VI) removal from river water. *Journal of Environmental Management*, 316, 115260.
- Goudu, M., Jitendra, K. S., Shraban, K. S., Ankita, D. and Yasvanti, C. (2024) Removal of congo red and malachite green from aqueous solution using ternary GO/Bi₂O₃/MgO materials by coprecipitation method. *Journal of Indian Chemical Society*, 101, 101323.
- 29. Dong, Y., Liang, J., Zhengyang, E., Song, J., Liu, C., Ding, Z., Wang, W. and Zhang, W. (2024) Preparation of biochar/iron mineral composites and their adsorption of methyl orange. *Royal Society of Chemistry*, **14**, 33977.
- 30. Ahmad, N., Kameda, T., Rahman, M. T. and Lesbani, A. (2025) Application and regeneration of magnetic material MgA1LDH@Fe₃O₄ humic acid with removal capacity for malachite green. *Inorganic Chemistry Communications*, **172**, 113669.
- 31. Cheng, Y., Li, A., Wei, S. and Zhao, L. (2024) Magnetic chitosan-functionalized waste carton biochar composites for efficient adsorption of anionic and cationic dyes. *Chemical Engineering Journal*, **481**, 148535.
- 32. Esra, K., Belgin, G., Berkant, K. and Dimitrios, K. (2017) Adsorption of malachite green on Femodified biochar: influencing factors and process optimization. *Desalination and Water Treatment*, 74, 383–394.
- 33. Xian, X., Feiyan, Z., Chenyu, Y., Lun, L., Yuan, Z., Baohua, T. and Liangzhong, L. (2025) Adsorption and reduction of Cr (VI) by C-P-O groups in biochar: performance and mechanisms. *Solid State Sciences*, **160**, 107815.
- 34. Mohamad, A. M. S., Dalia, K. M., Wan, A. W. A. K. and Azni, I. (2011) Cationic and anionic

- 79 Wan Noni Afida Ab Manan and Ahmad Zamani Ab Halim
 - dye adsorption by agricultural solid wastes: a comprehensive review. *Desalination*, **280**, 1–13.
- 35. Lincai, P., Jing, G., Xianqiu, L., Huaiping, L. and Hang, S. (2020) Modified ginkgo leaves for adsorption of methyl violet and malachite green dye in their aqueous system. *Desalination and Water Treatment*, **206**, 358–370.
- 36. Sun, M., Wang, C., Luo, Z. and Zhu, X. (2023) Synthesis of magnetic biochar with high iron content and large specific surface area:

- Synthesis, Characterization, and Adsorption Screening of Nanomagnetic Activated Carbon Derived from Biomass Waste: Oil Palm Trunk, Pinewood, and Rubberwood for the Removal of Malachite Green Dye Solution
 - synergistic effect of Fe doping and KOH activation. *Journal of Analytical and Applied Pyrolysis*, **173**, 106096.
- 37. Yalvac, G. M. and Bayrak, B. (2020) Use of natural and effective mandarin peel in elimination of malachite green from the aqueous media: adsorption properties, kinetics and thermos-dynamics. *Desalination and Water Treatment*, 177, 176–185.